

## **Emissions of Volatile Particulate Components from Turboshaft Engines Operated with JP-8 and Fischer-Tropsch Fuels**

**Meng-Dawn Cheng<sup>1\*</sup>, Edwin Corporan<sup>2</sup>, Matthew J. DeWitt<sup>3</sup>, Bradley Landgraf<sup>4</sup>**

<sup>1</sup> *Oak Ridge National Laboratory, Environmental Sciences Division, Oak Ridge, TN*

<sup>2</sup> *Wright-Patterson Air Force Research Laboratory, Wright-Patterson AFB, OH*

<sup>3</sup> *University of Dayton Research Institute, Dayton, OH*

<sup>4</sup> *Allegheny College, Meadville, PA*

---

### **Abstract**

Particulate emissions from two types of helicopter turboshaft engines operated with military JP-8 and paraffinic Fischer-Tropsch (FT) fuels were characterized as an objective of the field campaign held at the Hunter Army Airfield in Savannah, GA in June 2007. In general helicopter engines exhaust particles size distributions observed at the engine nozzle and 4.14 m downstream locations showing the geometric mean diameters smaller than 50 nm for all engine power settings investigated in this study. For both locations, the geometric mean diameter increased as the engine power setting increased; this trend also holds true for the emitted particle number concentration. The growth of particle geometric mean diameter was found significant, 7 nm, only in the case of the idle power setting.

Sulfur-to-sulfate conversion was found to be independent of the engine power setting. Emissions of both sulfur and sulfate increased as the engine power increased. When JP-8 fuel was used, particles smaller than 7 nm were found to increase in samples taken at the downstream location. The number concentration in this tail increased as the power setting increased. No such observation was found when FT fuel was used implying that the increased formation of nuclei particles in the plume downstream was likely to be caused by the sulfur and aromatic compounds in the JP-8 fuel. Total particulate carbon emissions increased as the engine power setting increased. Use of FT fuel reduced the elemental carbon emissions as it compared to the JP-8 fuel, and organic carbon emission at idle power but not at the higher powers. The reduction of elemental carbon by the FT fuel was attributed to the absence of aromatics (soot precursors) in the fuel. The OC/EC ratio was found to be in the range of 3-50 depending on the engine power setting. The aircraft emitted OC/EC was found to decrease as the engine power increased.

---

\* Corresponding author Tel: 1-865-241-5918;

Fax: 1-865-576-8646

E-mail address: chengmd@ornl.gov

**Keywords:** Aircraft; Engine particles; Fischer-Tropsch; JP-8; SMPS.

---

## INTRODUCTION

Vehicles with airbreathing engines, such as aircraft, are a major component in modern-day transportation. The aircraft engines operate with liquid hydrocarbon fuels, like typical ground-based vehicles; with some major differences in the combustion chamber design and emissions control (Lefebvre, 1999). Over the past 20 years, civilian air travel grew by an annual average of 4.8 percent. This was despite two major world recessions, terrorist acts, the Asian financial crisis of 1997, the severe acute respiratory syndrome (SARS) outbreak in 2003 and two Gulf wars. Based on Boeing's market prediction (<http://www.boeing.com/commercial/cmo/>), on average over the next 20 years, passenger travel will grow at 5.0 percent and cargo at 5.8 percent. The United States military uses approximately three billion gallons per year (~ 10% of total US aviation fuel use). The fleet average emission index for soot has been estimated to be approximately 40 mg/kg of fuel burned [International Civil Aviation Organization (ICAO) Data Base (<http://www.caa.co.uk/default.aspx?catid=702>)]. This in turn results in approximately 400,000 kg of particulate matter are emitted each year by US military aircraft alone.

It is anticipated that the increased demand on air travel will increase output of undesirable emissions, such as carbon monoxide (CO), carbon dioxide (CO<sub>2</sub>), nitrogen oxides (NO<sub>x</sub>),

sulfur dioxide (SO<sub>2</sub>), hazardous air pollutants (HAPs) like formaldehyde, 1,3-butadiene, acetaldehyde, acrolein, benzene, ethylbenzene, naphthalene, unburned hydrocarbons and particulate matter. Emissions of gaseous species (e.g., HAPs, CO, and unburned hydrocarbons) are generally much higher during idling, taxiing, and low engine power operations than that at the cruise or max power setting. Particulate matter (PM) emitted by aircraft are in the ultrafine particle-size region with the peak mobility diameter typically less than 100 nm (see Rogers *et al.*, 2005; Cheng *et al.*, 2008). These ultrafine particles undergo active transformation dynamics in the exhaust plume and possess very complex chemical composition. Unfortunately, there is currently no regulatory-certified method for sampling and measurement of aircraft turbine engine PM exhaust.

There are two types of PM in aircraft engine emissions that are of great concerns to human health and the environment. Primary PM is a class of non-volatile particles emitted directly from aircraft engines, which without additional sampling modification can be detected with particle instruments at the engine exhaust plane (EEP). These particles contain primarily soot and trace amount of metals. Secondary PM is formed through physical and chemical conversions of volatile and semi-volatile species (also called precursors) in the aircraft engine plume as it travels downstream of the EEP and cools and

interacts with ambient air. The Society of Automotive Engineers (SAE) E-31 committee recently published an Aerospace Information Report (AIR 5892, <http://www.sae.org/servlets/works/documentHome.do?comtID=TEAE31>) describing several methods for sampling and analysis of non-volatile particulate matter (i.e., soot) for aircraft emissions measurement. Volatile particles cannot be detected at the EEP according to the SAE-E31 AIR 5892.

Current knowledge regarding the volatile components in aircraft turbine engine emissions at ground level indicates that these are composed of two major classes of chemical species – sulfur and carbon-containing compounds (e.g., Petzold and Schröder, 1998; Wong *et al.*, 2008). Species within these two classes play active roles in chemical reactions and aerosol microphysics. For instance, soot particles are known to be hydrophobic and contain almost no water-soluble materials (Wyslouzil *et al.*, 1994; Petzold and Schröder, 1998). Adsorption of sulfuric acid agglomerates and molecular clusters (formed through nucleation, for instance) could occur inside a jet exhaust plume in the atmosphere (Miake-Lye *et al.*, 1994; Kärcher, 1996) leading to chemically modified soot particles that become hydroscopic with improved light-scattering efficiency. Frenzel and Arnold (1994) reported that the formation of sulfite in the plume is only restricted to plumes of age less than 10 ms. Gas-to-particle conversion and coagulation that lead to the buildup of sulfuric acid-water clusters would produce particles of about 1 nm in size within a plume of age about

0.5 s. Subsequent growth is by sulfuric acid condensation, coagulation, and further uptake of water vapor molecules. An alternative path of sulfate formation is catalytic oxidation of sulfur dioxide molecules in water droplets containing carbonaceous particles (e.g., Dlugi *et al.*, 1981; Mamane and Gottlieb, 1989). Sulfur dioxide molecules have to be transported to water droplets, which is diffusion limited. This conversion path is time-consuming (> 1 hr) and also requires high water vapor content; it may be important only for aged aircraft exhaust in humid atmosphere.

Rotating-wing aircraft (helicopters) are a major vehicle by the US military for air-lifting of cargo and personnel. Civilian uses of helicopters are also wide-spread. Emissions data of rotating-wing aircraft are scarce; only a limited number of literature references are identified for military helicopter emissions (Corporan *et al.*, 2004; Wade, 2004; Rogers *et al.*, 2005; Chen *et al.*, 2006; Jones *et al.*, 2007) reported measurement of polynuclear aromatic hydrocarbons (PAHs) from a UH-1H helicopter and found the emissions level of PAHs is comparable to that of diesel engine exhaust. Corporan *et al.* (2007) conducted a comprehensive study characterizing non-volatile particulate and gaseous emissions of a turboshaft T63 engine operating on a Fischer-Tropsch (FT) derived fuel. This study reports measurement results of volatile particulate emissions on two major helicopter engines used by the US Army. Comparisons of volatile PM emissions from the T700-class engines operating on conventional JP-8 and a

paraffinic FT fuel will be discussed. We also analyze and report the relationships of carbon and sulfur – based particles with respect to the engine operating condition.

## MATERIALS AND METHODS

The helicopter emissions measurement campaign was conducted at the Hunter Army Airfield (HAAF) in Savannah, GA in June, 2007. Two types of turboshaft engines (T700-GE-700 and T700-GE-701C) that are commonly used on military helicopters, such as the Blackhawk and Apache, were focused. The 700-GE-701C (called T701C hereafter) is a newer and improved version of T700-GE-700 (called T700 engine hereafter). Attributes characterized in this campaign for the turboshaft engine emissions include, for particulate phase, engine smoke number (SN) (which currently is the only accepted method by SAE), particle size distribution, number and mass concentrations, sulfate, and carbon and elemental (including sulfur) concentrations, and for gas phase, concentrations of carbon monoxide (CO), carbon dioxide (CO<sub>2</sub>), nitrogen oxide (NO), nitrogen dioxide (NO<sub>2</sub>), total hydrocarbons (THC), and selected organic species listed by the US Environmental Protection Agency as hazardous air pollutants. Filter samples were collected and analyzed for organic and elemental carbon, and total elemental sulfur and sulfate data were also taken in addition to several elements/metals. Besides filter data and smoke number, all other data were continuous measurements. Open-path optical

remote sensing methods for emissions measurement were also explored during this field campaign. The results will be reported separately.

A photograph taken during the T700/T701C engine emission test is shown in Fig. 1(a). The extractive sampling probes were mounted in a vertical rake with the probe tips approximately 40.6 cm downstream of the engine nozzle. A vertical plane at the distance of the probe tip is called the engine exhaust plane or EEP. Fig. 1(b) shows a close-up look of the sample probes mounted on the stainless steel rake. Three tip-dilution probes were used for particle samples, three undiluted probes were used for gas sampling, and two thermocouples were used for measurement of exhaust plume temperature. Each probe was separated by 3.18 cm center-to-center. The particles were diluted with nitrogen gas immediately at the probe tip upon sampling (Cheng *et al.*, 2008; Corporan *et al.*, 2008). The diluted and undiluted probes had the same probe geometry and inlet diameter.

Bundled sampling lines were used to transfer the engine exhaust from the probes to the instruments located in a trailer (called trailer 1) approximately 23 m from the probe rake. The bundled line from the probe tips to the valve box (not shown in Fig. 1(a)) was maintained at 150°C and the line temperature from the valve box to the trailer 1 was maintained at 75°C to prevent condensation of water vapor and condensable organics within the sampling lines. Continuous particle measurements in trailer 1 included a TSI, Inc.

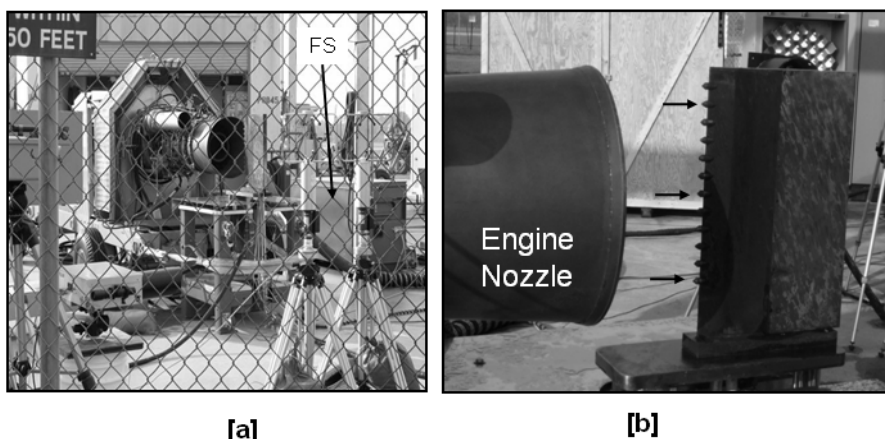


**Fig. 1.** A photo showing the field setup for helicopter engine emissions measurement at HAAF (a) and close-up of the tip-dilution sampling probes mounted on a vertical stainless steel rake in front of the engine nozzle (b).

Scanning Mobility Particle Sizer (SMPS<sup>®</sup>), a condensation particle counter, a smoke sampler, and a Taper-Element Oscillation Microbalance (TEOM). One of the sampling lines from the rake (Fig. 1(b)) was connected to the box labeled as FPS in Fig. 1(a), where a prototype fastscan particle sizer (FPS) was located. The sampling distance between the probe tip and the fastscan inlet was approximately 0.9 m. The FPS data will be discussed in a separated paper (Mahurin *et al.*, 2008) and not used in this paper.

A second rake containing two probes was located 4.14 m downstream from the engine nozzle. These probes were not diluted because the engine plume was naturally diluted in the environment. These probes, termed “environmental probes”, were used to provide extractive samples for instruments and samplers located in trailer 2. The rake for the environmental probes was located outside of the fence surrounding the test facility (shown as the dotted line in Fig. 2), but the probe tips were located inside the fence to prevent

contamination caused by particles previously deposited on the screened fence. The relative locations of the sampling rakes, trailers, and the engine in the test cell facility are shown in Fig. 2. The residence time for the plume to reach the tip of the environmental probe varied from 180 ms to 550 ms depending on the engine power setting.

The particle size distribution was measured at both locations (i.e., EEP and 4.14 m downstream) via simultaneous use of several differential mobility analyzer- (DMA) based instruments, including two sets of TSI SMPS<sup>®</sup>. One was equipped with a long DMA (model 3081) and TSI model 3022 CPC and located in trailer 1. The sample to this instrument was supplied by one of the extractive tip-dilution probes and drawn via vacuum to the instrument through the heated sampling system described in detail in Cheng *et al.* (2008) and Corporan *et al.* (2008). The other SMPS was equipped with a nano DMA (model 3085) and TSI model 3025A and located in trailer 2. The sample to this

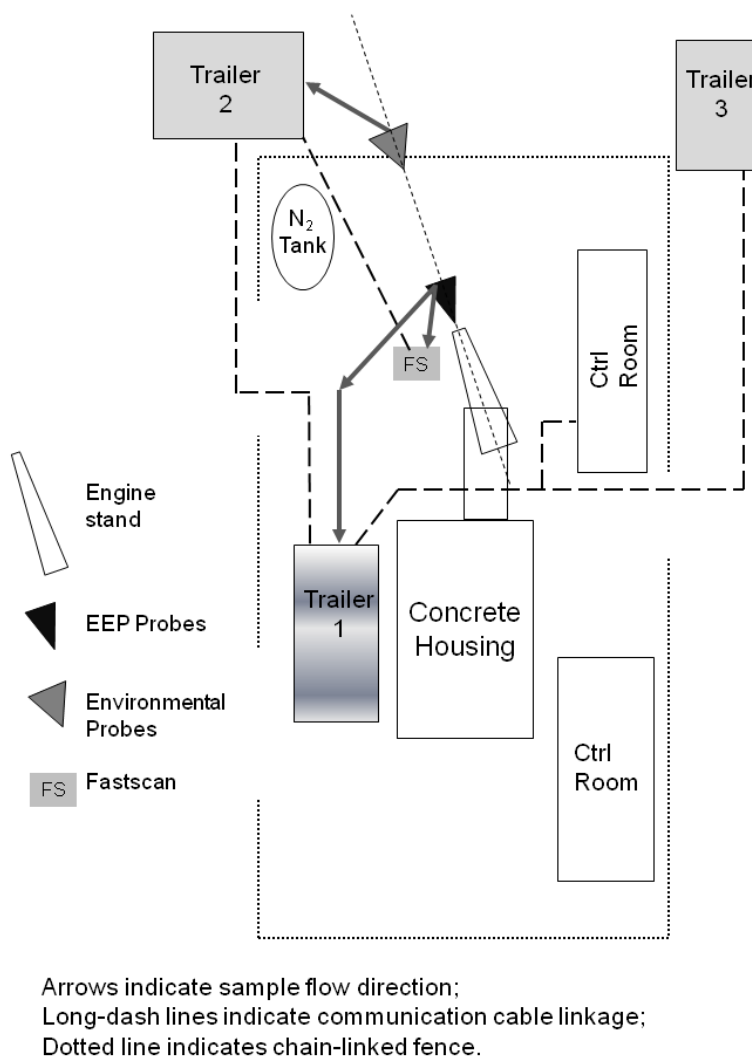


**Fig. 2.** Relative locations of trailers, control rooms, fastscan instrument, probes, and various installations to the engine test stand at HAAF. The dotted center line connects the center line of the engine nozzle (on the engine stand), the EEP probes, and the environmental probes.

instrument was supplied by one of the environmental probes through an unheated sampling line of about 21 m in length. The measurement cycle for a particle size distribution by the two SMPS instruments was 60 s up-scan and 30 s down-scan for a total measurement cycle time of 90 s.

A sandwiched PM-1 impaction-style sampler operated at 23 standard liters per minute was used to collect samples on pre-conditioned quartz filters; the particles

collected are those that have aerodynamic diameter less than or equal to 1.0  $\mu\text{m}$ . Depending on the engine power setting, the sampling duration for carbon and sulfur/elements varied between 5 to 10 min. After collection, the quartz filters were removed from the sampling train, Paraflex<sup>®</sup>-sealed in a filter container and stored at room temperature. The filters were analyzed following the NIOSH 5040 protocol (<http://www.cdc.gov/niosh/nmam/pdfs/5040f3>

.pdf) for diesel particulate matter on a Sunset Laboratory carbon analyzer (Birch and Cary, 1996). Field blank filters were analyzed by the same procedure as the samples and the averaged blank was subtracted from the data to yield the final carbon results. The time-integrated carbon samples collected in trailer 2 were analyzed back at Oak Ridge National Laboratory after the campaign.

The sulfur and sulfate analyses were performed on a second set of filter samples collected using a second PM-1 sampler operated at the same flow rate and sampling duration. The sample media for elements and sulfate were TEFLO<sup>®</sup> filter. Field blank filters were analyzed for background correction. Since the elemental sulfur was measured by non-destructive XRF technique, the same filter was used to analyze for sulfate by using ion chromatography. Most elemental concentrations were near or below detection limits; thus, they are not reported here. The same filters were then analyzed by ion chromatograph (IC) for sulfate analysis following the XRF analysis. The XRF sulfur data provide a total elemental sulfur content of the filter collected particles, while the IC data provide a total sulfate.

The two filter data sets described above provided time-integrated data for sulfur, sulfate, organic and elemental carbons that are representative of aircraft emission at steady-state engine operation for a given power setting. The time-integrated techniques, although reliable, may be inadequate to describe aircraft emissions during transients, which this study did not address. Three engine

power settings, idle, 75% max continuous and max continuous power were tested successively in a single test cycle. The information on fuel flow, turbine speed, and engine temperature were obtained from the HAAF facility personnel. Two to three cycles were repeated for each engine, yielding a total of 30 test points for the campaign. Military JP-8 fuel was used primarily throughout this campaign for a T700 and two T701C engines, while one of the T701C engines was also tested with 100% paraffinic Fischer-Tropsch (FT) fuel using the same test-cycle design.

## RESULTS AND DISCUSSION

### *Fuel Analysis*

The JP-8 and FT fuels used in the engine tests were sampled and analyzed for JP-8 specification properties. The fuel-analysis results are shown in Table 1. The FT fuel is composed solely of iso- (82%) and normal (18%) paraffins with a distillation range similar to a typical JP-8. Details on the physical and chemical aspects of this fuel have been previously reported (Corporan *et al.*, 2007a; 2007b; DeWitt *et al.*, 2007). Several fuel properties (e.g., heat of combustion, freeze point, and hydrogen content) were observed to be fairly similar between the two fuel types. It is important to note that the FT fuel does not contain aromatics or sulfur in contrast to JP-8 (i.e., 19% by volume for aromatics and 0.14% by weight for sulfur); thus, the formation of secondary PM in the experiments with FT fuel was expected to be negligible.

**Table 1.** Composition analysis results of JP-8 and FT fuels used in the HAAF campaign.

| ASTM TEST ITEM                     | STANDARD    | JP-8  | NEAT FT FUEL |
|------------------------------------|-------------|-------|--------------|
| Aromatics, % vol (D1319)           | Max. 25.0   | 19.2  | 0.00         |
| Total Sulfur, % wt (D4294)         | Max. 0.3    | 0.14  | 0.00         |
| Initial Boiling Point, °C (D86)    | Report      | 173   | 150          |
| 10% Recovered, °C (D86)            | Max. 205    | 189   | 173          |
| 20% Recovered, °C (D86)            | Report      | 192   | 181          |
| 50% Recovered, °C (D86)            | Report      | 207   | 208          |
| 90% Recovered, °C (D86)            | Report      | 234   | 245          |
| Final Boiling Point, °C (D86)      | Max. 300    | 248   | 258          |
| Distillation-Residue, % vol (D86)  | Max. 1.5    | 1.30  | 1.50         |
| Loss, % vol (D86)                  | Max. 1.5    | 1.50  | 0.50         |
| Freeze Point, °C (D5972)           | Max. -47    | -51   | -49          |
| Existent Gum, mg/100mL (D381)      | Max. 7.0    | 1.1   | 0.6          |
| Viscosity @ -20°C, cSt (D445)      | Max. 8.0    | 5.0   | 4.9          |
| FSII (DiEGME), % vol (D5006)       | 0.10-0.15   | 0.12  | 0.05         |
| Smoke Point, mm (D1322)            | Min. 19.0   | 25.0  | 35.0         |
| Flash Point, °C (D93)              | Min. 38.0   | 62.0  | 63.0         |
| Specific Gravity @ 15.5°C (D4052)  | 0.775-0.840 | 0.806 | 0.756        |
| Heat of Combustion, BTU/lb (D3338) | Min. 18400  | 18500 | 18980        |
| Hydrogen Content, % mass (D3343)   | Min. 13.4   | 13.7  | 15.3         |

### **Particle Size Distributions**

The shape of size distributions of particle in T700 and T701C engine emissions are similar to those displayed in Fig. 3. As an example, the averaged particle size distributions observed at the EEP for the T700 engine operated with JP-8 fuel for the three power settings are displayed in Fig. 3(a), which shows the geometric mean diameter (GMD) was generally less than 50nm for all three distributions. Also noted in Fig. 3(a) that the particle concentration at GMD and the GMD of a distribution both increased as the engine power increased. The GMD of the particles increased from 20nm at the idle power to 42nm at the max power. The variation in the

number concentration of each distribution shown in Fig. 3(a) is approximately  $\pm 10$ -15% of the average and independent of the engine power setting.

The averaged particle size distributions sampled by the environmental probe for the same three power settings are also displayed in Fig. 3(b) for comparison with those obtained at the EEP. The distributions in Fig. 3(b) were corrected for plume dilution using the ratio of CO<sub>2</sub> concentrations measured by the EEP probe to that measured by the environmental probe. The overall pattern of the two groups of particle size distribution shown in Figs. 3(a) and 3(b) are similar. In Fig. 3(b) from the environmental probe, the GMD and particle

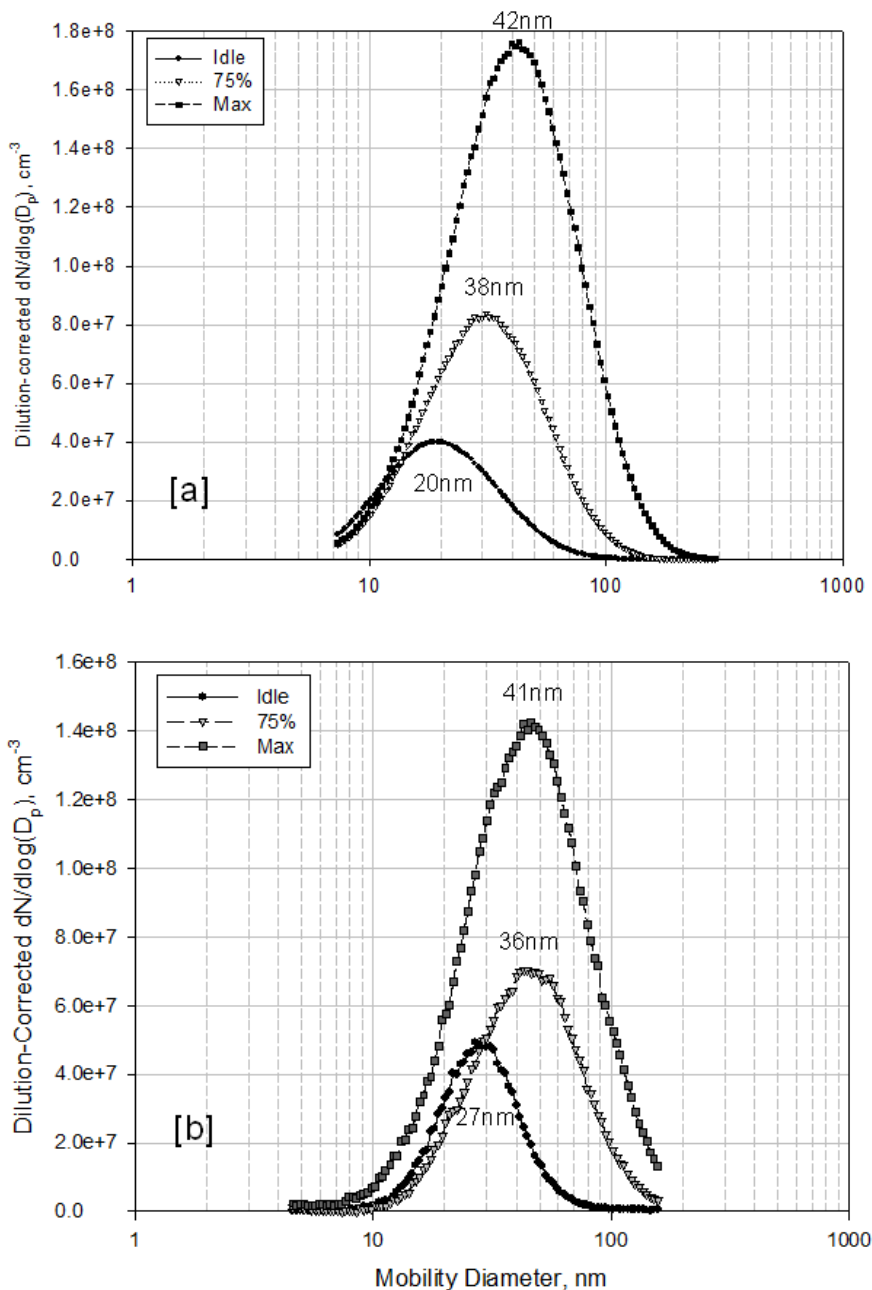


**Fig. 3.** Average particle size distributions for T700-JP8 emissions measured for three engine power settings (the idle, 75% or 75% max and max) at the EEP (a) and the 4.14 m location downstream (b).

concentration increased again as the engine power increased as those found at the EEP. In contrast, the GMD value at the idle power condition as shown in Fig. 3(b) was increased by approximately 7nm from that shown in Fig. 3(a). The growth defined by GMD increase was found to be minimal, if any, for the two

higher engine-power settings. There was 2nm growth in the GMD at the 75% max power condition and 1nm at the max power condition. These growths were within the statistical fluctuations ( $\pm 5\%$  of the GMD) embedded in the measurements.

### ***Fuel Effect on the Formation of Nuclei Particles***

The left tail region of a measured particle size distribution displayed in Fig. 4 was magnified. All size distributions were on samples taken by the environmental probe and are dilution-corrected. Some of the distributions in Fig. 4 show an increased numbers of particles from the mobility diameter of 7nm and smaller; the upward trend in the number concentration as the engine power increased was most apparent in Figs. 4(a) and 4(b) when JP-8 fuel was used. In the FT case shown in Fig. 4(c), the upward tail was unclear for both the idle and 75% max conditions pointing to the critical role of fuel sulfur and aromatic hydrocarbons played in the formation of nuclei particles in aircraft emissions. At the max power of the FT case (in Fig. 4(c)), the curve did not show the upward pattern; instead, a small peak was found at 11nm. The source of this 11-nm peak was unclear because (1) there were no sulfur to form condensible sulfuric acid species and (2) most paraffinic hydrocarbons were burned completely at the max power. Without aromatic hydrocarbons in the FT fuel, much less soot was produced in the T701C-FT max power case (see Fig. 8(a)). So, it is plausible from the data displayed in Fig. 4(a), 4(b) and 4(c), the formation of the upward-tail section of an engine particle size distribution could be primarily attributed to the sulfur and aromatics in the JP-8 fuel.

### ***Particulate Sulfur***

The sulfur data for the emissions of T700

engine running JP-8 fuel are displayed in Fig. 5. The sulfur and sulfate data were corrected for plume dilution using the same dilution ratio mentioned previously for particle size distribution. For testing with FT, the sulfur emissions were below the analytical detection limits and are thus not reported in this paper. The three solid bars in Fig. 5 show the total elemental sulfur content of the particles for the three engine power settings, while the three open bars show the sulfur content derived from the sulfate measurement on the same particles. The sulfur in sulfate [designated as S(IV) in this paper] was calculated by multiplying the measured sulfate concentration by a molecular weight ratio of (32/96). As shown in Fig. 5, both sulfur and sulfate concentrations increased as the engine power was increased from the idle to the max setting. The data also show that difference between the elemental sulfur and the S(IV) contents was statistically insignificant. In other words, all the particulate sulfur on the filter samples was analytically sulfate in our study.

Oxidation of SO<sub>2</sub> to the oxidized sulfur form like sulfate, bisulfate, or sulfite in the atmosphere is well-understood (e.g., Brasseur *et al.*, 1999; Seinfeld and Pandis, 1998). Current understanding indicates oxidation can take place in the gas or liquid phase. The gas phase takes place by addition of OH radical to SO<sub>2</sub>, with a rate coefficient of 9E-13 (cm<sup>3</sup>/molecule/s) at atmosphere. Sulfur trioxide (SO<sub>3</sub>) then reacts with water molecules in the gas phase or gets uptake into droplets to form sulfuric acid. Sulfuric acid

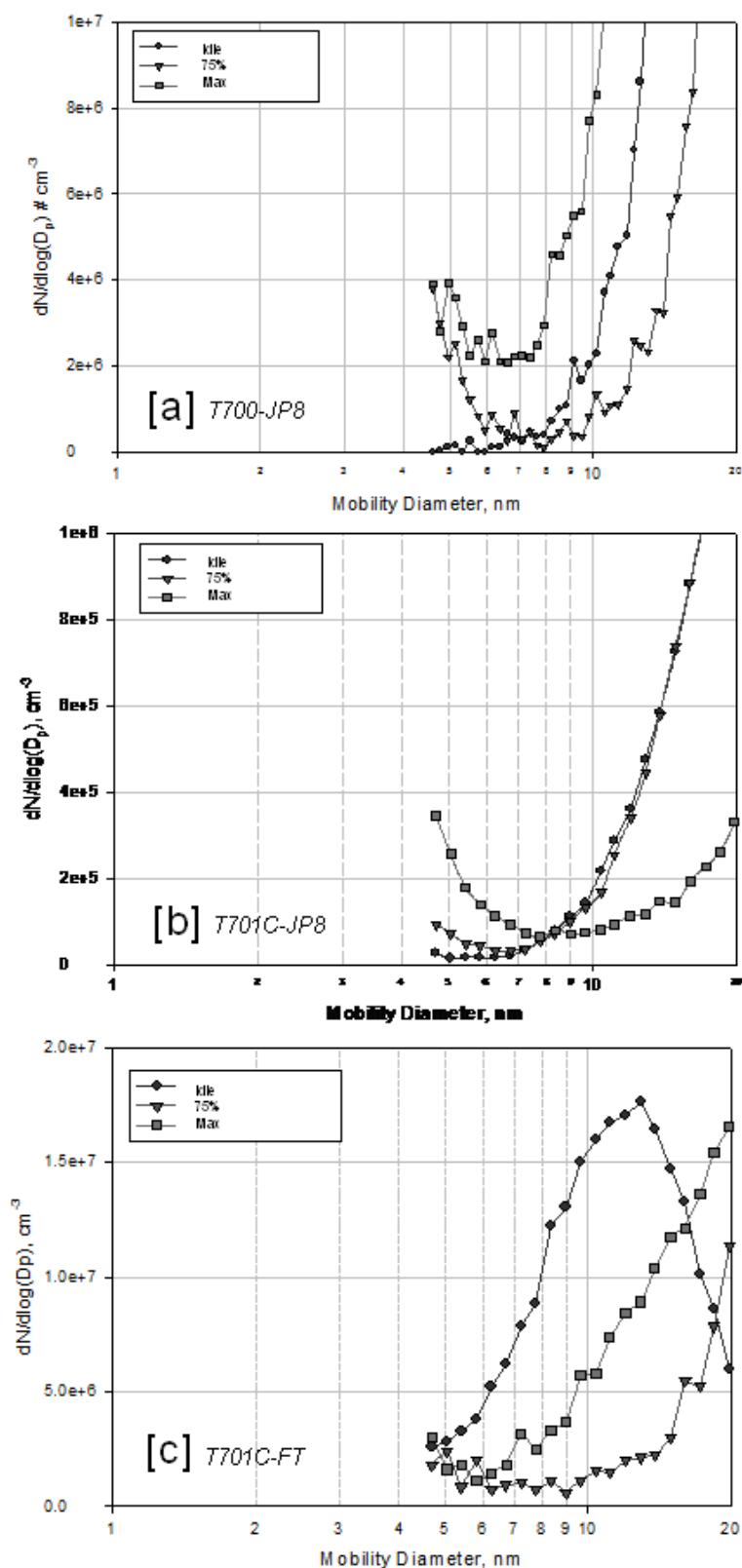


**Fig. 4.** Magnified plots of average particle size distributions for mobility diameter smaller than and equal to 20 nm for three engine power settings. (a) is for T700 engine operated with JP-8, (b) is for T701C engine operated with JP-8, and (c) is for T701C engine operated with FT fuel.

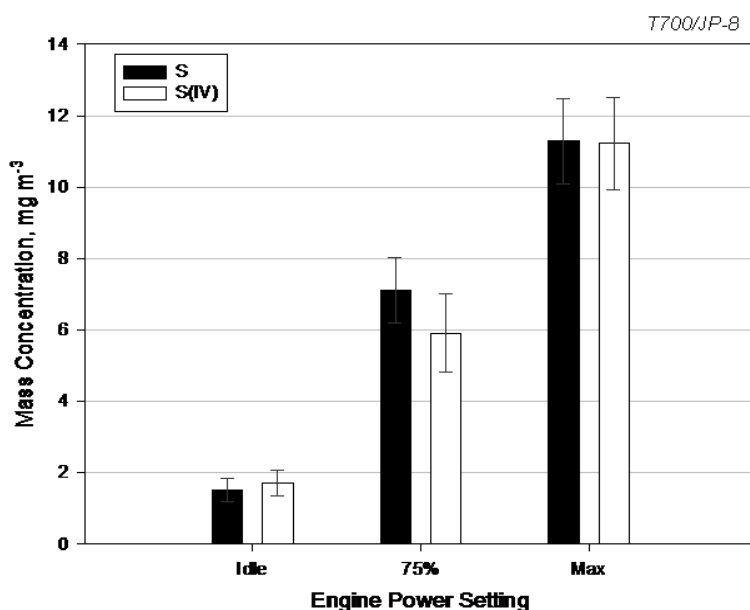


**Fig. 5.** Total particulate sulfur measured by XRF and total sulfur in SO<sub>4</sub> form [or denoted as S(IV)] measured by IC as a function of engine power setting. Sulfur and sulfate data are from T700-JP8 exhaust samples taken at the environmental probe.

then is taken up by other droplets or form new droplets if the local condition is favorable to nucleation. The pH of droplets in the plume controls the solubility of SO<sub>2</sub> and liquid-phase oxidation that could involve ozone, OH, HO<sub>2</sub>, and several transition metal ions like Fe or Ni commonly found in atmospheric aerosols. However, it is worth noting that sulfur conversion was indicated to be greater than that explained by our current knowledge of contrail physics and chemistry (DeWitt, 2003).

With the estimated residence time of 550 ms at the idle power to 180 ms at the max condition between the EEP and the environmental probe tip, the T700/T701C engine plumes cannot be considered as young (< 10 ms) plumes based on the previous findings (Frenzel and Arnold, 1994; Kärcher *et al.*, 1995; Petzold and Schröder, 1998). On the other hand, the age of particles in all test

cases in this study were not as old as those of the ambient particles (~hours to days), either. There was little liquid water droplets present in the plume. Thus, one likely mechanism for fuel sulfur to be converted to sulfate in the plume was that the gas-phase sulfur dioxide oxidation. SO<sub>2</sub> was formed in the engine combustor, then reacts with •OH or singlet •O radicals to form SO<sub>3</sub> species in the plume which subsequently reacts with water molecules in the air or on the surface soot particles to form H<sub>2</sub>SO<sub>4</sub>. Alternatively, SO<sub>3</sub> could react with water molecules in the vapor phase to form sulfuric acid that collide and combine with soot particles in the turbulent plume flow.

Using the T700-JP8 data, two plots were made to Fig. 6 show (1) the relationship between the sulfur-in-sulfate/total sulfur ratio [S(IV)/S] and engine power setting and (2) the

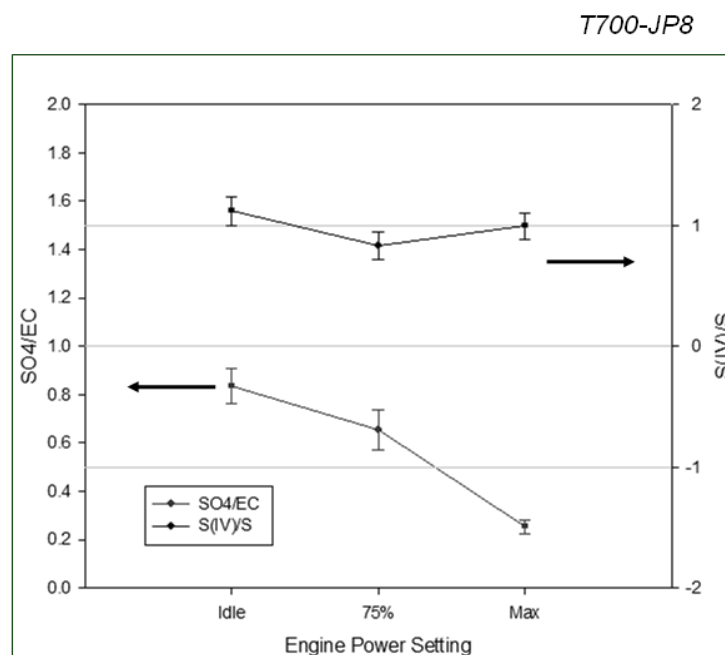


**Fig. 6.** Relationship between sulfate/total sulfur and sulfate/elemental carbon and the three engine power settings in T700/T701C-JP8 exhaust. Sulfur, sulfate, and carbon samples were taken by the environmental probe.

relationship between the sulfate/elemental carbon (EC) ratio and engine power setting. The S(IV)/sulfur ratio at the three engine power settings is reasonably close to the value of one, which again indicates that the conversion of sulfur to sulfate in the T700-JP8 plume was independent of the engine power setting. The sulfate to EC ratio decreased from 0.8 to 0.2 as the engine power setting was increased from the idle to the max, supporting the reaction mechanism of sulfur conversion (Petzold and Schroder, 1998; Kärcher and Yu., 2009).

### **Particulate Carbon**

Using a PM-1 sampler similar to that used to sample particle sulfur and sulfate, particulate carbon was measured on a separate

set of filter samples from those for sulfur taken at the environmental probe downstream from the EEP. The particulate carbon data were corrected for plume dilution using the same dilution ratio mentioned previously for particle size distribution and sulfur/sulfate.

The total particulate carbon emission increased as the engine power setting increased as shown in Fig. 7, consistently, for all three engine-fuel combinations (i.e., T700-JP8, T701C-JP8, and T701C-FT). The T700-JP8 emits the highest particulate carbon content, while the use of FT fuel (in the T701C-FT case) significantly reduced particulate emissions over the range of conditions studied. The total carbon emission by T701C-JP8 is less than that of T700-JP8 because the T701C engine is a newer model

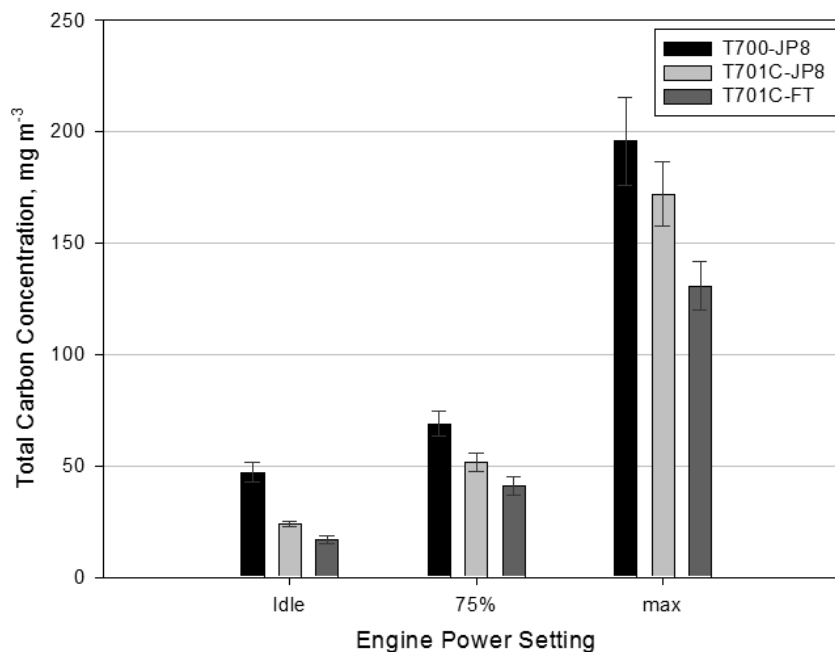


**Fig. 7.** Particulate carbon emissions as a function of engine power setting. The carbon samples were taken at the environmental probe.

and just serviced before this campaign. The reduction in particulate carbon emission is most likely attributed to the absence of particulate precursors (sulfur and aromatics) in the FT fuel (see Table 1). The absence of aromatics results in significant reduction of the fraction of EC in the soot (Corporan *et al.*, 2007).

Operational breakdown of the total particulate carbon into elemental and organic carbon (i.e., EC and OC) leads to investigate the formation of soot and non-soot fractions in the carbon emission. In general the higher engine power leads to higher EC emission that is consistent across different engine and fuel. The relationship between EC and the engine power setting is similar to that found for total particulate carbon shown in Fig. 7. The EC was negligible when FT fuel was used in the T701C engine operated at the idle and 75%

max power settings. Even comparing the three bars of the T701-FT with those of the T700-JP8 and T701C-JP8 the reduction of elemental carbon (EC) mass concentration shown in Fig. 8(a) was substantial, some 50%-85% by average. Also noticed in Fig. 8(a) is the dramatic increase in the EC emission from the 75% max power to the max power setting.

The emission of organic carbon as shown in Fig. 8(b) was more complicated than those of the EC in Fig. 8(a). In general the OC emission consistently increases as the engine power increases for all three engine-fuel cases. The reduction in the OC emission at the idle power setting by the FT fuel is observed in Fig. 8(b), but not for the other two higher power settings. In the 75% max power setting, the emissions of T701C engines (with JP-8 and FT) are lower than that of the T700-JP8, but both OC emissions of T701C engines are

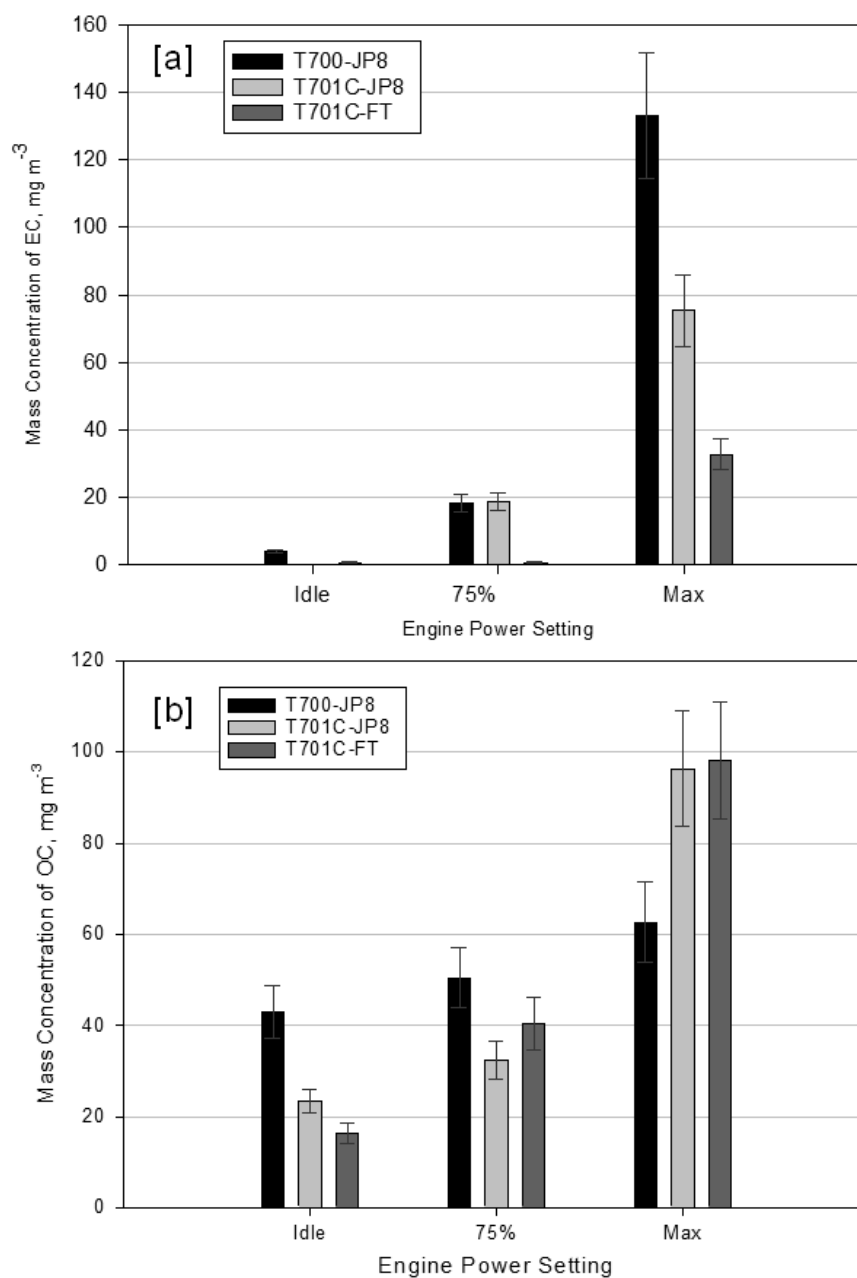


**Fig. 8.** Plot of particulate elemental carbon concentration ( $\text{mg}/\text{m}^3$ ) as a function of engine power setting is displayed in (a). The organic carbon (OC) as a function of engine power setting is displayed in (b).

statistically identical. In the max power setting, the emissions of two T701C engines are however higher than that of the T700 engine. Again, two OC emissions by the two T701C engines at the max power conditions are statistically identical.

#### ***Ratio of OC to EC***

The ratio of OC to EC has been used to interpret data on secondary aerosol formation and to trace/distinguish emission sources (e.g., He *et al.*, 2004; Chu, 2005; Jaffrezo *et al.*, 2005; Aymoz *et al.*, 2006). For instance, He *et*

*al.* (2005) found that average OC/EC ratio was 2.4, 4.2, 5.0 and 6.6 for Beijing, Gwangju, Kyoto and Ulaan-Battor, respectively. Jaffrezo *et al.* (2005) found the OC/EC ratio was in the range of 5 and 50 in the aerosols measured in the French Alps. Jaffrezo *et al.* (2005) also reported the size-resolved OC/EC ratio and found most particles smaller than 50 nm have OC/EC ratios greater than 10. In these works, the ratio was considered a useful indicator for distinguishing the primary organic carbon from the secondary one. To our knowledge, there is no such OC/EC ratio for aircraft emission as a function of engine power. Fig. 9 shows the relationship between OC/EC and the engine power setting for the engine and fuel. The trend shows that the ratio decreased as the engine power increased for a given engine-fuel combination. Since OC measured in our study was mostly in the near field of

aircraft emission, we have doubt about significant formation of secondary organic compounds as compared to the primary OC emitted by the engine. Thus, primary OC tends to increase as the engine power increased as shown in Fig. 8(b).

The increase of primary OC slows down as the power increased from the idle to the 75% max in Fig. 8(b), as compared to those of EC shown in Fig. 8(a). The OC/EC ratio is therefore expected to decrease as the engine power increased. This is exactly shown in Fig. 9 for T700-JP8 and T701C-JP8. It is unknown at the present on the cause of the large bar associated with the T701C-FT at 75% max power. Without this outlier, the OC/EC ratio for T701C-FT at the idle power is larger than that at the max power, which trend is consistent with the rest of the results of T700-JP8 and T701C-JP8. Also since the EC value

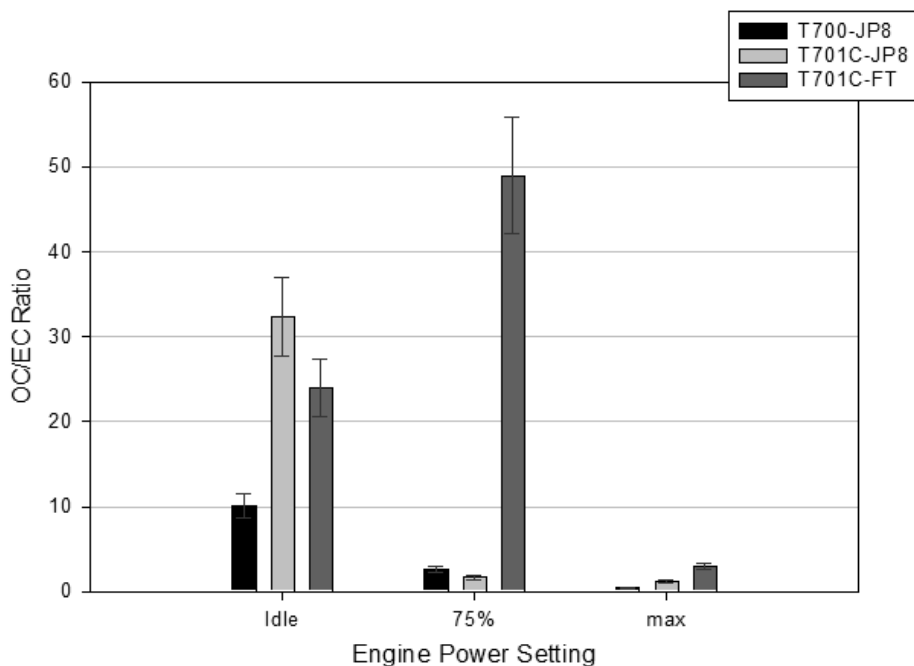


**Fig. 9.** Plot of OC/EC as a function of engine power setting. OC stands for organic carbon and EC stands for elemental carbon.

for T701C-FT at 75% was small (see Fig. 8 (a)); it is possible that dividing a small number would result in a large outlying OC/EC ratio as shown in Fig. 9.

## CONCLUSIONS

Particulate emissions from two types of helicopter turboshaft engines operated with military JP-8 and paraffinic Fischer-Tropsch (FT) fuels were characterized as an objective of the field campaign held at the Hunter Army Airfield in Savannah, GA in June 2007. In general helicopter engines exhaust particles size distributions observed at the engine nozzle and 4.14m downstream locations showing the geometric mean diameters smaller than 50nm for all engine power settings investigated in this study. For both locations, the geometric mean diameter increased as the engine power setting increased; this trend also holds true for the emitted particle number concentration. The growth of particle geometric mean diameter was found significant, 7nm, only in the case of the idle power setting.

Sulfur-to-sulfate conversion was found to be independent of the engine power setting. Emissions of both sulfur and sulfate increased as the engine power increased. When JP-8 fuel was used, particles smaller than 7nm were found to increase in samples taken at the downstream location. The number concentration in this tail increased as the power setting increased. No such observation was found when FT fuel was used implying that the increased formation of nuclei particles

in the plume downstream was likely to be caused by the sulfur and aromatic compounds in the JP-8 fuel. Total particulate carbon emissions increased as the engine power setting increased. Use of FT fuel reduced the elemental carbon emissions as it compared to the JP-8 fuel, and organic carbon emission at idle power but not at the higher powers. The reduction of elemental carbon by the FT fuel was attributed to the absence of aromatics (soot precursors) in the fuel. The OC/EC ratio was found to be in the range of 3 to 50 depending on the engine power setting. The aircraft emitted OC/EC was found to decrease as the engine power increased.

## ACKNOWLEDGEMENTS

This project was supported by the Department of Defense Strategic Environmental Research and Development Program (SERDP) under the project number WP1401 led by Oak Ridge National Laboratory (ORNL). The field campaign was supported by the aircraft maintenance crew in the Aviation Branch at the Hunter Army Airfield (HAAF) in Savannah, GA, and was greatly appreciated. In particular, we thank Joseph D. Lukas, Jr., who was a project officer/COR, Chief, Aviation Branch, Maintenance Div., DOL at HAAF. We also acknowledge the professional support by Daniel Houck, Robert Henson, Jason Mikelonis and Robert Shell who led the maintenance crew at the test facility. We also express our appreciation to the hospitality of personnel of the Department of Environmental

Protection on the HAAF installation. Shannon M. Mahurin (SMM) of ORNL participated in the campaign. Liyuan Liang and SMM contributed to the technical review of this paper. Oak Ridge National Laboratory is managed by UT-Battelle, LLC, for the U.S. Dept. of Energy under contract DE-AC05-00OR22725.

## DISCLAIMER

Mention of trade names, chemicals and instrument model and model number in this paper should not be construed as endorsement or recommendation by the Oak Ridge National Laboratory and the Wright-Patterson Air Force Research Laboratory.

## REFERENCES

- Aymoz, G., Jaffrezo, J.L., Chapuis, D., Cozic, J. and Maenhaut W. (2006). Seasonal Variation of PM<sub>10</sub> Main Constituents in Two Valleys of the French Alps. I: EC/OC Fractions. *Atmos. Chem. Phys.* 6: 6211-6254.
- Birch, M.E. and Cary, R.A. (1996). Elemental Carbon-Based Method for Monitoring Occupational Exposure to Particulate Diesel Exhaust. *Aerosol Sci. Technol.* 25: 221-241.
- Brasseur, G.P., Orlando, J.J. and Tyndall, G.S. (1999). *Atmospheric Chemistry and Global Change*, Oxford University Press, New York.
- Chen, Y.C., Lee, W.J., Uang, S.N., Lee, S.H. and Tsai, P.J. (2006). Characteristics of Polycyclic Aromatic Hydrocarbon (PAH) Emissions from a UH-1H Helicopter Engine and Its Impact on the Ambient Environment. *Atmos. Environ.* 40: 7589-7597.
- Cheng, M.D., Corporan, E., DeWitt, M., Klingshirn, C. and Mahurin, S.M. (2008). Characterization of Rotating-Wing Aircraft Emissions, Paper #208, Presented at the National Meeting of Air and Waste Management Association, Portland, OR, June.
- Chu, S.H. (2005). Stable Estimate of Primary OC/EC Ratios in the EC Tracer Method. *Atmos. Environ.* 39: 1383-1392.
- Corporan, E., Quick, A. and DeWitt, M.J. (2008). Characterization of Particulate Matter and Gaseous Emissions of a C-130H Aircraft. *J. Air Waste Manage. Assoc.* 58: 474-483.
- Corporan, E., DeWitt, M.J., Klingshirn, C.D. and Striebich, R.C. DOD Assured Fuels Initiative: B-52 Aircraft Emissions Burning a Fischer-Tropsch/JP-8 Fuel Blend. *Proceed. 10<sup>th</sup> Int'l Conf. on Stab. and Hand. of Liq. Fuels.* 2007b.
- Corporan, E., DeWitt, M.J. and Wagner, M. (2004). Evaluation of Soot Particulate Mitigation Additives in A T63 Engine. *Fuel Process. Technol.* 85: 727-742.
- Corporan, E., DeWitt, M.J., Belovich, V., Pawlik, R., Lynch, A.C., Gord, J.R. and Meyer, T.R. (2007a). Emissions Characteristics of a Turbine Engine and Research Combustor Burning a Fischer-Tropsch Jet Fuel. *Energy Fuels.* 21: 2615-2626.
- Chen, D.R., Pui, D.Y.H., Hummes, D., Fissan,

- H., Quant, F.R. and Sem, G.J. (1998). Design and Evaluation of a Nanometer Aerosol Differential Mobility Analyzer (Nano-DMA). *J. Aerosol Sci.* 29: 497-509.
- DeWitt, K.J. (2003). *Sulfur Oxidation and Contrail Precursor Chemistry*, NASA/CR-212293.
- DeWitt, M.J., Striebich, R., Shafer, L., Zabarnick, S., Harrison III, W.E., Minus, D.E. and Edwards, T. (2007). Evaluation of Fuel Produced Via the Fischer-Tropsch Process for Use in Aviation Applications. Paper 58b, Proc. of AIChE Spring National Meeting.
- Dlugi, R., Jordan, S. and Lindemann, E. (1981). The Heterogeneous Formation of Sulfate Aerosols in the Atmosphere. *J. Aerosol Sci.* 12: 185-197.
- Frenzel, F. and Arnold, F. (1994). Sulfuric Acid Cluster Ion Formation by Jet Engines: Implications for Sulfuric Acid Formation and Nucleation, Rept. DLR Mitt. 94-06, Dtsch. Forsch. Für Luft-und Raumfahrt, Köln, Germany.
- He, Z., Kim, Y.J., Ogunjobi, K.O., Kim, J.E. and Ryu, S.Y. (2004). Carbonaceous Aerosol Characteristics of PM<sub>2.5</sub> Particles in Northeastern Asia in Summer 2002. *Atmos. Environ.* 38: 1795-1800.
- Jaffrezo, J.L., Aymoz, G. and Cozic, J. (2005). Size Distribution of EC and OC in the Aerosol of Alpine Valleys during Summer and Winter. *Atmos. Chem. Phys.* 5: 2915-2925.
- Jones, X.L., Penko, P.F, Williams, S. and Moses, C., Gaseous and Particle Emissions in the Exhaust of a T700 Helicopter Engine. Proceedings of the ASME Turbo Expo Conference, GT2007-27522, 2007.
- Kärcher, B. (1996). Aircraft-Generated Aerosols and Visible Contrails. *Geophys. Res. Lett.* 23: 1933-1936.
- Kärcher, B. and Yu, F. (2009). Role of Aircraft Soot Emissions in Contrail Formation. *Geophys. Res. Lett.* 36: L01804, doi:10.1029/2008GL036649.
- Kärcher, B., Peter, Th. and Ottmann, R. (1995). Contrail Formation: Homogeneous Nucleation of H<sub>2</sub>SO<sub>4</sub>/H<sub>2</sub>O Droplets. *Geophys. Res. Lett.* 22: 1501-1504.
- Lefebvre, A.H. (1999). *Gas Turbine Combustion*, 2<sup>nd</sup> Ed., Edwards Brothers, Ann Arbor, MI.
- Mahurin, S.M., Corporan, E., De Witt, M.J. and Cheng, M.D. (2008). Fast Time Scale Measurement of Particulate Matter from Military Helicopter Engines. Submitted to *Environ. Sci. Technol.* October.
- Mamane, Y. and Gottlieb, J. (1989). The Study of Heterogeneous Reactions of Carbonaceous Particles with Sulfur and Nitrogen Oxides Using a Single Particle Approach. *J. Aerosol Sci.* 20: 575-584.
- Miake-Lye, R.C., Brown, R.C., Anderson, M.R. and Kolb, C.E. (1994). Calculations of Condensation and Chemistry in an Aircraft Contrail, Rept. DLR Mitt. 94-06, Dtsch. Forsch. Für Luft-und raumfahrt, Köln, Germany.
- Petzold, A. and Schröder, F.P. (1998). Jet Engine Exhaust Aerosol Characterization, *Aerosol Sci. Technol.* 28: 62-76.
- Rogers, F., Arnott, P., Zielinska, B., Sagebiel, J., Kelly, K.E., Wagner, D., Lighty, J.S. and

- Sarofim, A.F. (2005). Real-Time Measurement of Jet Aircraft Engine Exhaust. *J. Air Waste Manage. Assoc.* 55: 583-593.
- Seinfeld, J.H. and Pandis, S.N. (1998). *Atmospheric Chemistry and Physics: From Air Pollution to Climate Change*, J. Wiley & Sons, Inc., New York.
- Wade, M.D. (2004). Aircraft/Auxiliary Power Units/Aerospace Ground Support Equipment Emission Factors, USAF Report IERA-RS-BR-SR-2003-0002.
- Wong, H.W., Yelvington, P.E., Timko, M.T., Onasch, T.B., Miake-Lye, R.C., Zhang, J. and Waitz, I.A. (2008). Microphysical Modeling of Ground-Level Aircraft-Emitted Aerosol Formation: Roles of Sulfur-Containing Species. *J. Propul. Power.* 24: 590-602.
- Wyslouzil, B.E., Carleton, K.L., Sonnenfroh, D.M., Rawlins, W.T. and Arnold, S. (1994). Observation of Hydration of Single, Modified Carbon Aerosols. *Geophys. Res. Lett.* 21: 2107-2110.

*Received for review, November 25, 2008*

*Accepted, January 12, 2009*